한국소음진동공학회지 제 10 권 제 6 호, pp. 1048~1058, 2000.

〈논 문〉

Hybrid Technique for Active Vibration Control of Plate using Piezoceramic Actuators/Sensors

압전 작동기/감지기를 이용한 평판의 혼합형 능동 진동제어 기술

Yeung-Shik Kim*, Chul Lee** and Insoo Kim*
김 영 식 · 이 철 · 김 인 수

(Received April 26, 2000 ; Accepted October 30, 2000)

Key Words : Active Control(능동제어), Piezoelectric Actuator/Sensor(압전 작동기/센서), MIMO System Identification(다중 입출력계의 규명), Hybrid Controller(혼합형 제어기)

ABSTRACT

Thipaper presents a methodology to suppress the vibration of thin rectangular plate clamped all edges using piezo-ceramic material as actuators and sensors. Dynamic characteristics of the structure bonded with distributed actuators/sensors are identified by the Multi-Input Multi-Output (MIMO) frequency domain modeling technique based on the experimental data. Hybrid control scheme is adopted and feedback controller is designed by LQG(Linear Quadratic Gaussian). Feedforward controller is adapted by multiple filtered - x LMS(least mean square) algorithm. Experiment result demonstrates the effective reduction of the vibration label for both the transient and persistent external disturbances.

요 약

본 논문에서는 압전 세라믹 재료를 작동기 및 감지기로 이용한 사각 경계면이 고정된 얇은 사각평판의 능동 진동제어 방법을 제시한다. 실험 데이터에 기초한 다중 입출력계의 주파수영역 모델링방법을 이용하여 분포된 센서 및 구동기 특성이 포함된 구조물의 동적 특성이 규명된다. 제어기 구조로는 혼합형을 채택하고 되먹임 제어기는 LQG 제어기법에 의해 설계된다. 앞먹임 제어기는 다중 filtered- x 최소자승오차법에 의해 적응되도록 한다. 진동제어에 대한 시뮬레이션 및 실험결과는 제안된 제어기법이 지속적 외란 및 과도적 외란에 효율적으로 적용될 수 있음을 보인다.

1. Introduction

There have been many studies in the field of the active vibration suppression of structures using piezoelectric materials. Since piezoelectric material has high stiffness, good linearity, and easy of implementation, it is a good candidate for the structural vibration controls. The PZT ceramics can be used as actuators and sensors since they are compact and lightweight and do not need a support structure for reaction purposes. The effectiveness of the materials has been investigated in the control of structural vibrations[1,2], sound radiation/transmission[3~6], and noise and structural vibrations.[7]

In this study, modeling and control techniques are the main considerations for the vibration suppression of structures using PZT actuators and sensors. The theoretical modeling techniques of the structure bonded

* 정회원, 금오공과대학교 기계공학과
** 정회원, 금오공과대학교 대학원 기계공학과

with PZT have been developed[8,9]. However, they are generally very difficult or sometimes impossible to model the complex structures so that the experimental identification(ID) techniques are required. ID is the process of constructing a mathematical model of the system using experimental data to describe the input, output and noise relationship. The experimental ID can be divided into the time-domain and frequency-domain approaches. The experimental modeling technique by the state-space frequency domain identification[10] is introduced for the accurate model of complex shaped structures. This approach is much free from the MIMO model order problem caused at the digital implementation comparing with the other experimental identification techniques. The MIMO model includes reconstruction filters, power amplifiers, piezoelectric actuators/sensors, plate characteristics, and charge amplifiers in the modeling process.

In the control techniques, the control strategy is divided into the adaptive feedforward approach where the reference signal is needed and the feedback approach where the error signal only is used. In the adaptive feedforward approach, Widrow et al.[11] first proposed the filtered-x LMS algorithm. This method has the advantage of both its simplicity and the fact that error path dynamics does not have to be a minimum phase system[12]. R. J. Silcox et al.[13] addressed about the cylindrical enclosure by this approach. J. V. Warner et al.[14] applied RLMS algorithm to the three-dimensional acoustic enclosure and in recent study robust performance in persistent disturbance is achieved including the filtered-x and filtered-μ LMS algorithm.[15] Nelson et al.[16,17] developed a multiple error LMS algorithm which is a multi-channel generalization of the filtered-x LMS algorithm. However, when the reference signal related with the primary source is not available or reference signals are so many in the system, a feedback control approach can be considered. There have been many developed studies in the feedback approach. Recently the synthesized algorithm between the adaptive feedforward and feedback control is presented, and studies show that the adaptive feedforward controller with feedback loop is effective for the vibration reduction under both transient and stationary disturbances.[18,19]

The purpose of this paper is to present a methodology for the active vibration suppression of the thin panel using PZT actuators and sensors. For the effective vibration suppression, the adaptive feedforward with feedback loop based on the MIMO model, which is identified by the state-space frequency domain identification technique, is adopted. Since it has its robustness for both the transient and persistent external disturbances, and increases the convergence speed due to the reduced variance of the filtered-x signal by the feedback loop effect, i.e., increment of the structural damping. The adaptive feedforward control used is the well known multiple filtered-x LMS algorithm. The MIMO error path dynamics is controlled by the feedback loop, which is constructed by multivariable digital LQG controller composed of the regulator and Kalman filter. Experiment results are presented for the verification of the proposed approach and show the effective reduction of the vibration label for Gaussian random external disturbances.

2. System Identification

Because of the some limits of theoretical modeling for the practical implementation as notified before, the experimental identification process is introduced in this study. Under the consideration of the model order problem and more accurate model of MIMO system with frequency response functions, the frequency domain ID approach seems to be appropriate.

In this study, among many frequency domain ID methods, the method using the matrix-fraction rather rational matrix function for the curve fitting is adopted.[7] This method enables curve-fitting operation to be linear and requires no iteration calculation.

Now, let us consider the MIMO linear system of r inputs and m outputs. The transfer function of MIMO system in z-plane can be represented as follows:

$$G(z_k) = R(z_k)Q^{-1}(z_k) \tag{1}$$

where $R(z_k)$ and $Q(z_k)$ are the numerator and denominator matrices, respectively, and is the discrete-time transfer function matrix from the measured frequency response functions which are calculated in z-plane. Both and $R(z_k)$ can be

expanded as:

$$Q(z_k) = I_r + Q_1 z_k^{-1} + \cdots + Q_p z_k^{-p}$$
$$R(z_k) = R_0 + R_1 z_k^{-1} + \cdots + R_p z_k^{-p}$$
$$z_k = e^{j\frac{2\pi k}{l}} (k = 0, \cdots, l-1) \tag{2}$$

where I_r is an identity matrix of order r and every Q_i and R_i are $r \times r$ real square and $m \times r$ real rectangular matrices, respectively, and p is the order of the discrete-time transfer function.

Substituting equation (2) into equation (1) makes the transfer function $G(z_k)$ become

$$G(z_k) = -G(z_k)Q_1 z_k^{-1} - \cdots - G(z_k)Q_p z_k^{-p} + R_0 + R_1 z_k^{-1} + \cdots + R_p z_k^{-p} \tag{3}$$

because $G(z_k)$ is known at $z_k = e^{j\frac{2\pi k}{l}} (k = 0, \cdots, l-1)$ where the experimental frequency responses have its value at l frequency points from a spectrum analyzer, there are l equations available. For more general representation,

$$\Psi \simeq \Phi\Theta \tag{4}$$

where

$$\Phi = \begin{bmatrix} G(z_0)z_0^{-1} & \cdots & G(z_0)z_0^{-p} & I_m & z_0^{-1}I_m & \cdots & z_0^{-p}I_m \\ G(z_1)z_1^{-1} & \cdots & G(z_1)z_1^{-p} & I_m & z_1^{-1}I_m & \cdots & z_1^{-p}I_m \\ \vdots & \ddots & \vdots & \vdots & \vdots & \ddots & \vdots \\ G(z_{l-1})z_{l-1}^{-1} & \cdots & G(z_{l-1})z_{l-1}^{-p} & I_m & z_{l-1}^{-1}I_m & \cdots & z_{l-1}^{-p}I_m \end{bmatrix},$$

$$\Theta = \begin{bmatrix} -Q_1 \\ \vdots \\ -Q_p \\ R_0 \\ R_1 \\ \vdots \\ R_p \end{bmatrix}, \text{ and } \quad \Psi = \begin{bmatrix} G(z_0) \\ G(z_1) \\ \vdots \\ G(z_{l-1}) \end{bmatrix}$$

The least-square solution of Θ could be complex numbers. To avoid this, one can force Θ to be real by solving either the real part or the imaginary part of equation (4) in matrix notation, i.e.,

$$\begin{bmatrix} \mathrm{Re}(\Psi) \\ \mathrm{Im}(\Psi) \end{bmatrix} = \begin{bmatrix} \mathrm{Re}(\Phi) \\ \mathrm{Im}(\Phi) \end{bmatrix} \Theta \tag{5}$$

Therefore,

$$\hat{\Theta} = \begin{bmatrix} \mathrm{Re}(\Phi) \\ \mathrm{Im}(\Phi) \end{bmatrix}^{+} \begin{bmatrix} \mathrm{Re}(\Psi) \\ \mathrm{Im}(\Psi) \end{bmatrix} \tag{6}$$

where + represents pseudo-inverse and $\hat{\Theta}$ is the estimation of Θ. To apply the modern optimal control strategy, a state space form from the transfer functions can be written as

$$x(k+1) = Ax(k) + Bu(k), \quad y(k) = Cx(k) + Du(k) \tag{7}$$

where the system matrices A, B, C, and D are as follows:

$$A = \begin{bmatrix} 0 & I_r & 0 & \cdots & 0 \\ 0 & 0 & I_r & \cdots & 0 \\ \vdots & \vdots & \vdots & \ddots & \vdots \\ 0 & 0 & 0 & \cdots & I_r \\ -Q_p & -Q_{p-1} & -Q_{p-2} & \cdots & -Q_1 \end{bmatrix},$$

$$B = \begin{bmatrix} 0 \\ 0 \\ \vdots \\ 0 \\ I_r \end{bmatrix}, \quad C = \begin{bmatrix} R_p - R_0Q_p \\ R_{p-1} - R_0Q_{p-1} \\ \vdots \\ R_2 - R_0Q_2 \\ R_1 - R_0Q_1 \end{bmatrix}^T, \text{ and } \quad D = R_0$$

where the superscript T represents the matrix transpose.

3. Design of Active Vibration Control System

3.1 Adaptive Feedforward Control with Feedback Loop

Let us derive the multiple filtered-x LMS algorithm. Figure 1 represents the block diagram of the multiple filtered-x LMS algorithm. The error signal $e_n(k)$ at the $n-$th sensor is the sum of the disturbance and the secondary source signals. The error path dynamics, which includes low-pass filters, power amplifiers, PZT actuators/sensors, characteristics of the plate, and signal amplifiers, is represented by the finite impulse response (FIR) of the order p, i.e., $\boldsymbol{h}_{nm} = [h_{nm}(0), h_{nm}(1), \cdots, h_{nm}(p)]^T$. The FIR filter of the order q also represents the m-th adaptive controller, $\boldsymbol{w}_{m,k} = [w_{m,k}(0), w_{m,k}(1), \cdots, w_{m,k}(q)]^T$ which is where subscript k denotes the time step at which the filter coefficients are updated. The n-th error signal at the k-th step is as follows,

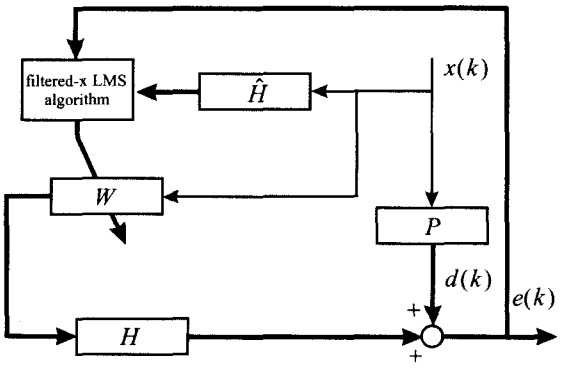

Fig. 1 Multiple filtered-x LMS algorithm

$$e_n(k) = d_n(k) - \sum_{m=1}^{M}\sum_{j=0}^{p}\sum_{i=0}^{q} h_{nm}(j) w_{m,k-j}(i) x(k-j-i) \tag{8}$$

where $d_n(k)$ is the vibration signal induced by the external disturbance. One of the optimal adaptive algorithms, the gradient descent method, is applied to find the global minimum value of the cost function $J = \sum_{n=1}^{N} e_n^2$ under the assumption that the coefficients of the controller are slowly changing.

$$\begin{aligned} w_{m,k+1}(i) &= w_{m,k}(i) + 2\mu(q+1)\sum_{n=1}^{N} e_n(k)\sum_{j=0}^{p} h_{nm}(j) x(k-j-i) \\ &= w_{m,k}(i) + 2\mu(q+1)\sum_{n=1}^{N} e_n(k) f_{nm}(k-i) \end{aligned} \tag{9}$$

Where μ is the convergence coefficient and $w_{m,k}(i)$ is the i-th coefficient of the m-th controller at the k-th sampling. This is the multiple filtered-x LMS algorithm having one reference input and the multiple error path dynamics. f_{nm} is the filtered-x signal which is obtained by passing the reference input through the error plant H_{mn}.

$$f_{nm}(k-i) = \sum_{j=0}^{p} h_{nm}(j) x(k-j-i) \tag{10}$$

Now, let us move onto the reason of inserting the feedback loop into adaptive feedforward controller. By applying Lyapunov stability criterion for the SISO case for the simple deduction, the convergence coefficient η is determined as follows[20],

$$0 < \eta < \frac{1}{\sum_{i=0}^{q} f^2(k-i)} \tag{11}$$

where η equals to $\mu(q+1)$. The stability criterion of iterative steepest descent algorithm may be summarized as follows[16].

$$0 < \eta < \frac{1}{(q+1)\sigma_f^2} < \frac{1}{\lambda_{\max}} \tag{12}$$

Since $\sum_{i=0}^{q} f^2(k-i)$ of equation (11) is equal to $(q+1)\sigma_f^2$ or $Tr(R_f)$ for the active control process under stationary random process, equation (11) may be approximated to the stability criterion of steepest descent algorithm. $Tr(R_f)$ and $\lambda_{\max}$ denote the trace and maximum singular value of auto-covariance matrix of filtered-x signal respectively. Equation (11) means that convergence coefficient of filtered-x LMS algorithm should be set inverse proportionally to the magnitude of filtered-x signal or impulse response of error plant H_{nm}. Therefore if external disturbance is consisted of the frequency components near to resonance of the error plant, feedforward controller adapted by filtered-x LMS algorithm would converge very slowly and be unsuitable for the control of frequently changing external disturbance.

In order to increase the convergence speed of the adaptive feedforward controller, a feedback controller may be used to improve the dynamics of error plant, such as increasing the damping capacity. This is the basic idea of proposed algorithm related with the design of hybrid controller. Note that when feedforward controller is combined with feedback loop, feedforward controller should be adapted based on the other filtered-x signal which is estimated using closed-loop transfer function $C = (I - HG)^{-1}H$ instead of error plant H. Equation (9) can be converted into the adaptation rule for multiple feedforward controllers with feedback loop,

$$w_{m,k+1}(i) = w_{m,k}(i) + 2\gamma\sum_{n=1}^{N} e_n(k)\sum_{j=0}^{p'} c_{nm}(j) x(k-j-i) \tag{13}$$

where FIR filter of p' order, $[c_{nm}(0), c_{nm}(1), \ldots, c_{nm}(p')]^T$ is impulse response weights of transfer function between m-th feedforward control signal and n-th residual vibration, namely the closed-loop transfer

function C_{nm}. Note that impulse response weights can be significantly less than ones of error plant $[h_{nm}(0), h_{nm}(1), \ldots, h_{nm}(p)]^T$ if feedback loop increases the damping capacity of error plant, and so convergence coefficient of the proposed algorithm γ can be set more greatly than η. Magnitude plot of closed-loop transfer function C_{nm} can make flat over interested frequency band by increasing damping ratio, and the condition number $\frac{\lambda_{\max}}{\lambda_{\min}}$ which is ratio between maximum and minimum singular values of covariance matrix of filtered-x signal by C_{nm} becomes close to one compared to the condition number by error plant H_{nm}. Because adaptation rate of filtered-x algorithm may be optimal when condition number is one[16], adaptation rate of hybrid controller can be improved. Therefore hybrid active controller may be able to attenuate even transient external disturbance as illustrated in later section by numerical simulation. Additionally, calculation burden for updating hybrid controller may be reduced because of $p' < p$.

3.2 Multivariable State Feedback Controller Design

The block diagram of the multiple adaptive feedforward control with feedback loop is shown in Fig. 2. In the feedback control of the error path, the Linear Quadratic Gaussian (LQG) algorithm is applied to the MIMO discrete error path model. Assuming that the MIMO model is stochastic linear system, the model is represented as follows,

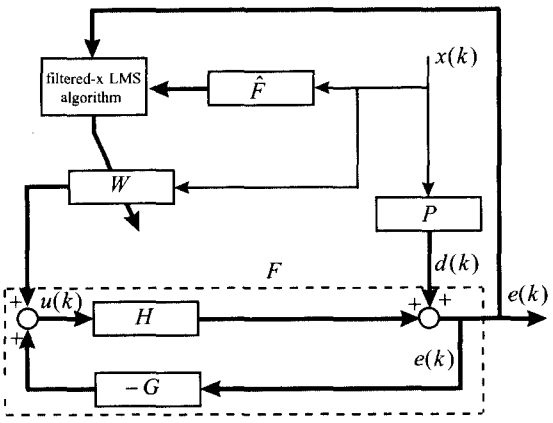

Fig. 2 Multiple adaptive feedforward control with feedback loop

$$x(k+1) = Ax(k) + Bu(k) + L\xi(k)$$
$$y(k) = Cx(k) + Du(k) + \theta(k) \quad (14)$$

where A, B, C and D are the system matrices, and L is the disturbace input matrice. And x, y and u are the state variable, the output and the control input, respectively. The process noise ξ and the measurement noise θ are assumed to be a stationary random process with zero-mean , the process noise covariance Q_o and measurement noise covariance R_o. The control input can be expressed as $u(k) = -MX(k)$, where M is the state feedback gain matrix that is determined by minimizing the performance index

$$J_d = \sum_{k=0}^{\infty} [x^T(k)Qx(k) + u^T(k)Ru(k)] \quad (15)$$

where Q is a real symmetric positive semi-definite matrix and R is a real symmetric positive definite matrix.

To get the state information $x(k)$ from the output $y(k)$, the Kalman filter is used and expressed as

$$\tilde{x}(k+1) = A\tilde{x}(k) + Bu(k) + K(y(k) - C\tilde{x}(k)) \quad (16)$$

where the gain matrix K is determined such that covariance of estimation error is minimized. In the LQG control method, weighting matrices R and Q, and the covariance matrices of the process and sensor noises Q_o and R_o are usually obtained by the trial-error. In this study, system matrices of state space representation is transformed into the modal canonical form where the complex eigenvalues appear in 2×2 blocks on the diagonal of the matrix A and real eigenvalues appear on the diagonal of the matrix A. Then, the state-weighting matrix Q is designed to have dominant values at 2×2 block diagonal terms. Weighting factors R, R_o and Q_o are adjusted repeatedly until the performance of feedback control system, such as increasing of damping capacity of error plant and disturbance reduction over the specified frequency band, is satisfied.

4. Simulation and Experimental Result

4.1 Simulation

Computer simulation is carried out in order to show which difficulties the filtered-x LMS algorithm possess and how those can be overcome by the proposed algorithm. Error plant is assumed to be the system with resonance at 65 Hz and 125.5 Hz as shown in Table 1. In general, primary plant is different from error plant because error plant involves the characteristics of actuator, low-pass filter and so forth, and external disturbance induced by primary source is transmitted to the sensors through different transmission paths. However it is assumed that primary plant is same with error plant except the added 3 step time-delay, i.e., z^{-3} for clarity of the simulation. LQG feedback controller is designed with such the weights as $R=1$, $Q=400C^T$, $R_o=1$ and $Q_o=400$. Figure 3 shows that closed-loop transfer function is significantly damped out at resonant frequencies compared to error plant. The convergence property for hybrid control is investigated under the harmonic disturbance. Figure 4 is the time signal of disturbance rejection related with feedback control, feedforward control and hybrid control in case that reference signal is consisted of sine wave of 65 Hz and one of 152.5 Hz changed abruptly from 0.8 second, and controller is initiated at 0.4 second. Performance of hybrid control was much better and faster compared to adaptive feedforward control and LQG feedback control. Note that even though LQG feedback controller has been designed under ideal condition, residual vibration by feedback controller cannot be eliminated completely. The result of feedforward control illustrates that filtered-x LMS algorithm yields poor transient response due to slow convergence rate. Simulation result shows that hybrid controller is able to recover quickly from transient disturbance because of active damping component of the control signal from feedback loop, and consequently performs better for both persistent and transient disturbances. As described in section (3.1), convergence pattern of filtered-x LMS and proposed algorithm depends on the condition number $\frac{\lambda_{max}}{\lambda_{min}}$ and the filtered-x signal power $Tr(R_f)$. The fact that $Tr(R_f)$ of filtered-x LMS is about 75 times as large as one of proposed algorithm and condition number of error plant with feedback loop is close to one compared to the condition number of uncontrolled error plant because magnitude plot of frequency

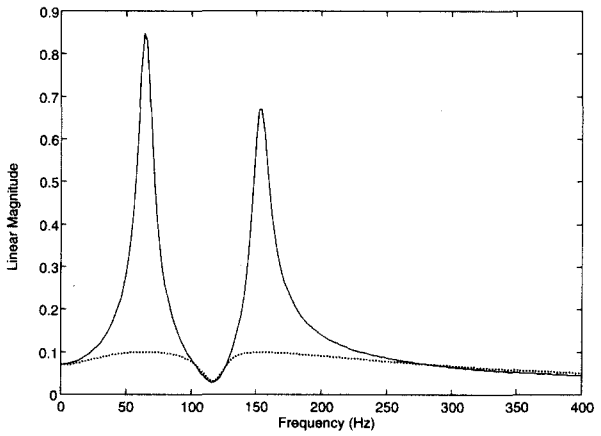

Fig. 3 Transfer functions for the error plant and the closed-loop system: ——— : Transfer function of the error plant; ----- : Closed-loop transfer function

Table 1 Computer simulation model of the error plant.

Zeros (z)	Poles (z)
0.9822±0.1456i	0.9742±0.1889i
0.9608	0.9902±0.0808i
Gain = 0.020221	

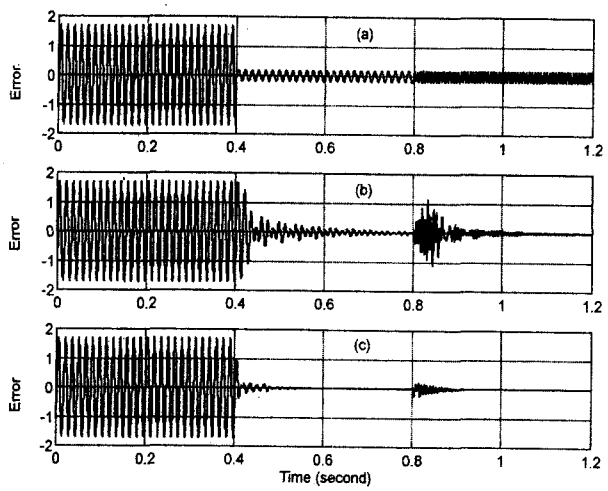

Fig. 4 Time histories of disturbance rejection. (a) LQG feedback control; (b) FXLMS algorithm; (c) Hybrid control

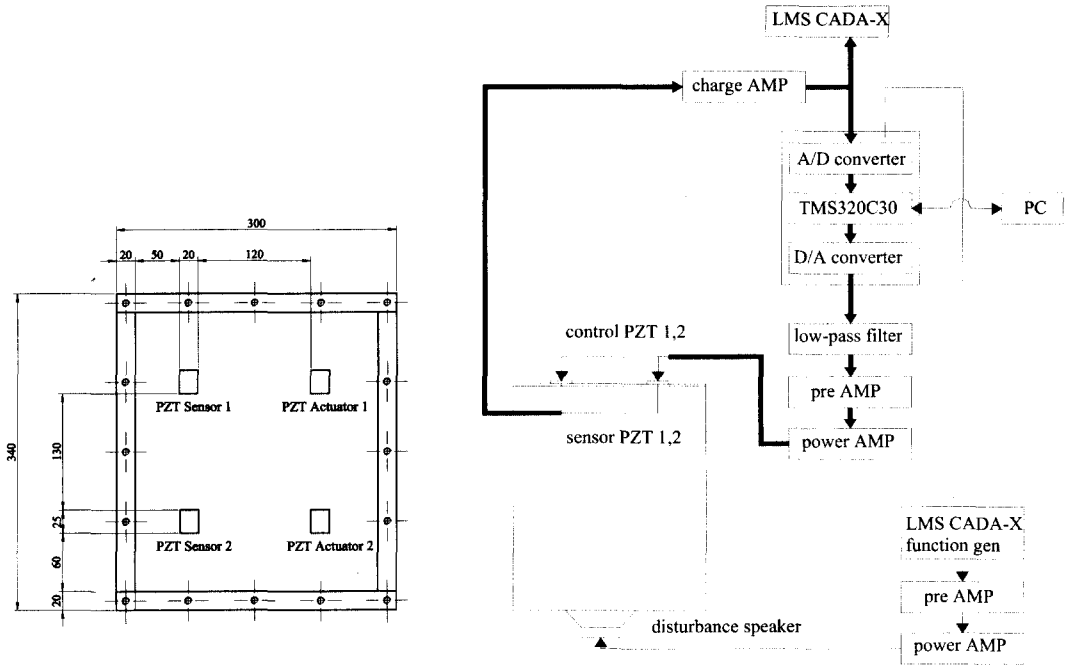

Fig. 5 Experimental setup

response function of error plant becomes flat over interested frequency band by active damping as shown in Fig. 3 supports this simulation result.

4.2 Experimental Setup

Figure 5 shows the experimental setup of the multiple adaptive feedforward control with feedback loop. The stainless steel plate of dimension 340×300×0.5(mm) clamped at all edges. To realize the vibration characteristics of plates, the plate is excited by the acoustic sound, which is generated by the speaker in the enclosure box. The acoustic natural frequencies of rectangular shape enclosure are higher than the plate vibration frequencies of our concern. The enclosure which has the inner dimension of 300×260×280 (mm) is surrounded by the 20 mm aluminum barrier. Two PZT sensors and two PZT actuators are placed at the centers of a quarter plane.

In the experimental modeling process, LMS CADA-X with Scadas II front-end and DI-2200 FFT analyzer are used for the frequency domain identification using the Gaussian random signal of the band of 85~185 Hz and the evaluation of the proposed control system. The adaptive feedforward controller with feedback loop is embodied on the digital signal-processing unit (Loughborough, TMS320C30 DSP) which has 12-bit 4 channel A/D converters and 12-bit 2 channel D/A converters with sampling rate of 0.8 kHz.

4.3 Experimental Result

In the modeling process of the error path dynamics including low-pass filters (cutoff frequency 220 Hz, order 3), power amplifiers (TECHRON 7540), PZT actuators/sensors, vibration characteristics of the plate, and charge amplifiers (B&K 2626), the 2×2 MIMO system model is experimentally identified in the form of the Auto-Regressive Moving-Average using four frequency response data. Through the persistent Gaussian random excitation, the frequency response data of error plants between PZT actuators and PZT sensors are obtained using FFT analyzer. Under the frequency domain identification procedure mentioned before, the MIMO model is obtained and realized on the state space.

Figure 6 shows the magnitude and phase comparisons between the measured and modeled frequency responses. A little difference between H12 and H21 in over 170 Hz frequency band may be due

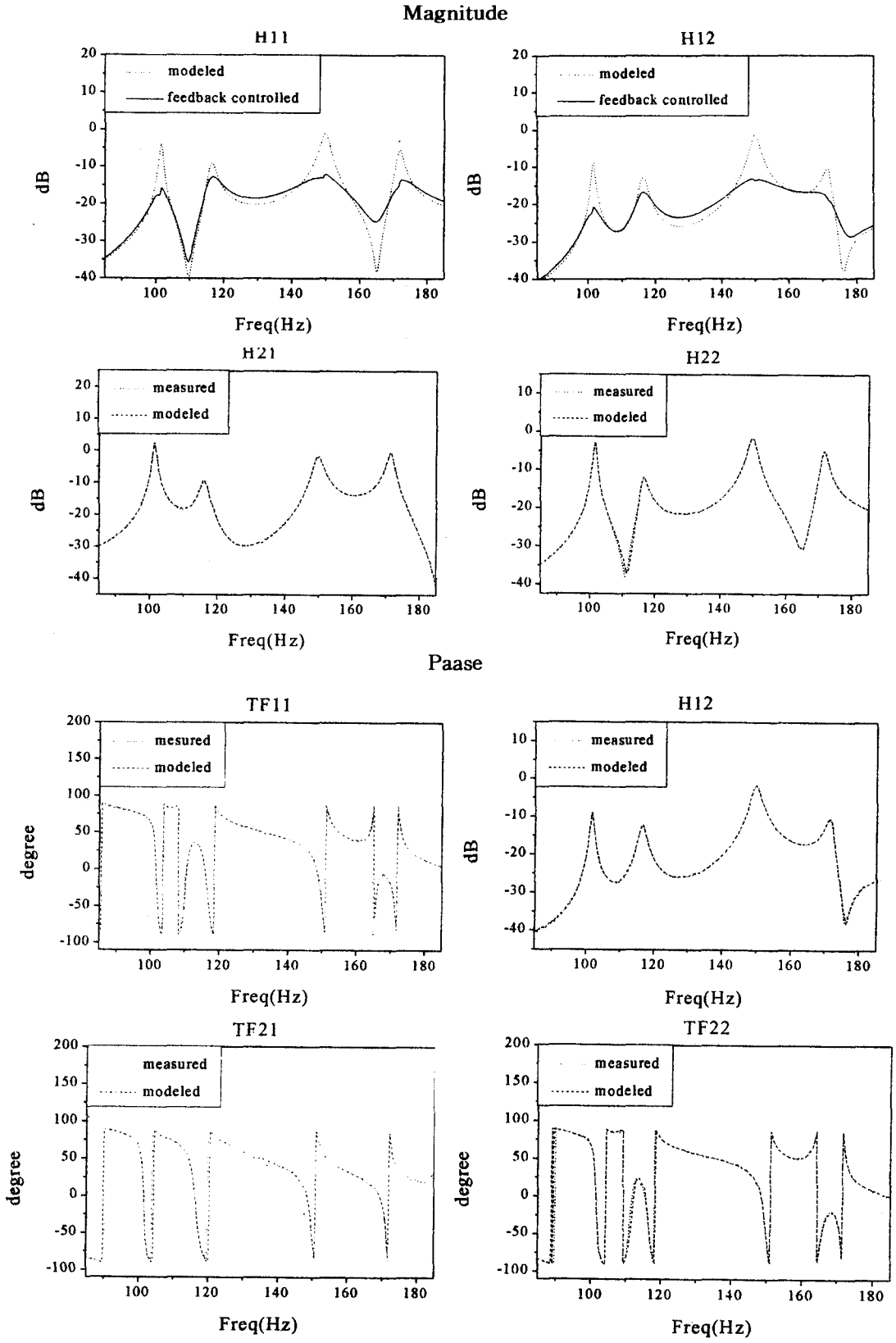

Fig. 6 Identification results of error path

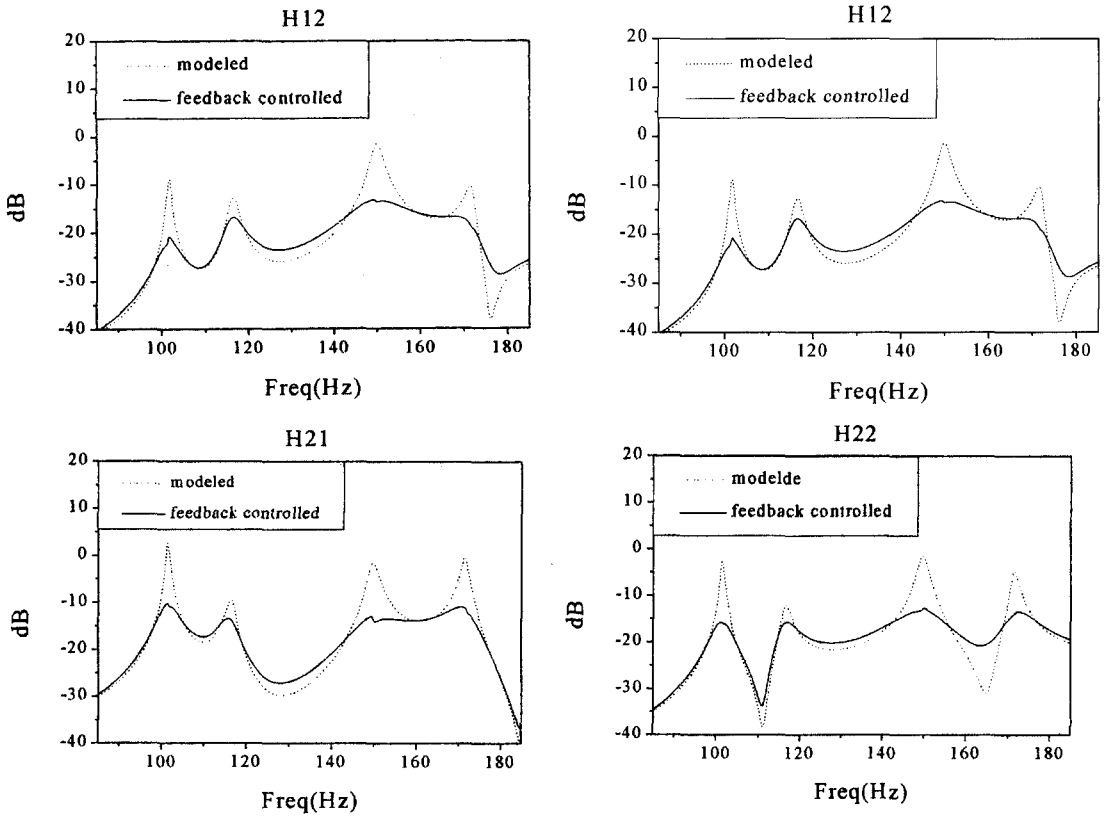

Fig. 7 Error path dynamics with feedback loop

to not uniform tensile load on plate induced during bolt mounting of plate. The model includes the four modes with the model order of 20. This MIMO model is very accurate as shown in this figure. However, the time-domain multivariable ARX(Auto-Regressive with exogenous input) modeling method resulted in the above 50 order with the same accuracy. Measured natural frequencies for each mode are 102 Hz, 117 Hz, 150 Hz, and 172 Hz, respectively.

The error plant is controlled using the LQG technique composed of the linear quadratic regulator and the Kalman filter. Table 2 shows that the damping ratios of feedback controlled error plant are 11~26 times as large as ones of uncontrolled error path. Solid lines in Fig. 7 represent the error path dynamics controlled by the feedback. Fig. 7 shows that magnitude of frequency response function of error plant becomes flat over interested frequency band by increasing damping ratio, and so adaptation rate of hybrid controller may be improved compared to the

Table 2 Dominant poles in z-plane, damping ratios of error plant and feedback controlled error plant.

Pole (uncontrolled)	0.6951± 0.7139i	0.6040± 0.7854i	0.3795± 0.9139i	0.2190± 0.9667i
Pole (controlled)	0.6462± 0.6386i	0.5389± 0.7147i	0.3247± 0.7957i	0.2084± 0.8224i
Damping ratio (uncontrolled)	0.0046	0.0101	0.0089	0.0066
Damping ratio (controlled)	0.1222	0.1190	0.1269	0.1233

feedforward controller as described in section (3.1) and section (4.1).

In the experimental implementation, the IIR-type digital controller can cause instability, because the used DSP unit allows only the six places under floating point. Therefore, the FIR-type is appropriate, where the order of 64 is selected after enough decay of impulse response of controller. Figure 8 shows spectrum results at the PZT sensor 1 with different control

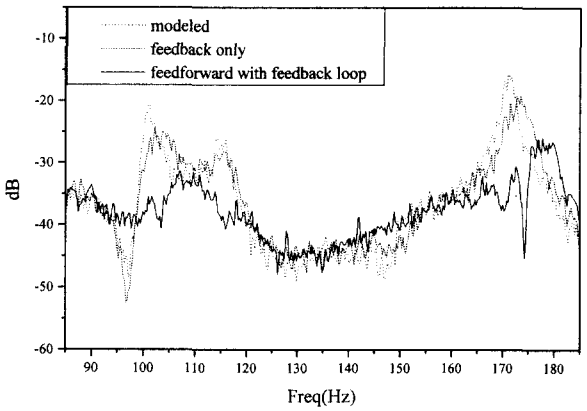

Fig. 8 Power spectrums at PZT sensor

status. Under the excitation of the plate by acoustic sound with 85~185 Hz Gaussian random noise, spectrums of the vibration level at PZT sensor 1 are measured. The 150 Hz peak is not presented in spectrums of the vibration level. This may be due to the acoustic field characteristics in enclosure because 150 Hz peak at PZT sensor 1 is presented when plate is excited by the outside sound wave from an external speaker and a standing wave at 150 Hz may be induced in enclosure. It is observed that reductions of the vibration level with the feedback loop and the adaptive feedforward control with feedback loop is 5dB and 15dB, respectively.

5. Conclusion

Multiple adaptive feedforward control approach with the feedback loop has been presented to suppress the vibration level of the plate using piezoelectric actuators and sensors. The problem of filtered-x LMS algorithm is analyzed theoretically in the viewpoint of convergence rate especially when error plant has resonant characteristics. Adding damping to the error plant by the feedback loop makes the convergence time be short and the resultant controller be effective to transient external disturbances due to high convergence coefficient. Simulation result demonstrates the effective reduction of the vibration label and the robustness for both the transient and persistent external disturbances. Effectiveness of the experimental modeling technique, i.e., the state-space frequency domain method, is examined. Experimental result shows that about 15 dB suppression of the vibration level across the first four modes in the rectangular plate may be accomplished using the proposed control scheme.

References

(1) Bailey, T. and Jr. Hubbard, J. E., 1985, "Distributed Piezoelectric-Polymer Active Vibration Control of a Cantilever Beam", J. of Guidance Control and Dynamics, 8(5), pp. 605~611.

(2) Tzou, H. S. and Tseng, C. I., 1990, "Distributed Piezoelectric Sensor/Actuator Design for Dynamic Measurement/Control of Distributed Parameter Systems : A Piezoelectric Finite Element Approach", J. of Sound and Vibration, 130(1), pp. 17~34.

(3) D'Cruz, J., 1995, "Global Multivariable Vibration Control with Distributed Piezoceramic Actuators", J. of Intelligent Material System and Structures, Vol. 6, pp. 419~429.

(4) Fuller, C. R., Hansen, C. H. and Snyder, S. D., 1991, "Experimental on Active Control of Sound Radiation from a Panel Using a Piezoceramic Actuator", J. of Sound and Vibration, 150(2), pp. 179~190.

(5) Snyder, S. D., Tanaka, N. and Kikushima, Y., 1995, "The Use of Optimally Shaped Piezo~electric Film Sensors in the Active Control of Free Field Structural Radiation, Part 1 : Feedforward Control", ASME J. of Vibration and Acoustics, Vol. 117, pp. 311~322.

(6) Snyder, S. D., Tanaka, N. and Kikushima, Y., 1996, "The Use of Optimally Shaped Piezo-electric Film Sensors in the Active Control of Free Field Structural Radiation, Part 2: Feedback Control", ASME J. of Vibration and Acoustics, Vol. 118, pp. 112~121.

(7) Sun, J. Q., Norris, M. A., Rossetti, D. J. and Highfill, J. H., 1996, "Distributed Piezoelectric Actuators for Shell Interior Noise Control", ASME J. of Vibration and Acoustics, Vol. 118, pp. 676~681.

(8) Wang, X., Ehlers, C. and Neitzel, M., 1996, "Dynamic Analysis of Piezoeletric Actuator Bonded on Beam", Third ICIM/ECSSM, pp. 883~890.

(9) Cole, D. G., Saunders, W. R. and Rovertshaw, H. H.,

1995, "Modal Parameter Estimation for Piezostructures", ASME J. of Vibration and Acoustics, Vol. 117, pp. 431~438.

(10) Juang, J. N., 1994, Applied System Identification, Prentice Hall.

(11) Widrow, B. and Stearns, S. D., 1985, Adaptive Signal Processing, Prentice Hall.

(12) Ren, Wei. and Kumar, P. R., 1989, "Adaptive Active Noise Control : Structures, Algorithms and Convergence Analysis", Inter-Noise, Newport Beach, CA, USA, pp. 435~440.

(13) Silcox, R. J., Lester, H. C. and Abler, S. B., 1989, "An Evaluation of Active Noise Control in a Cylindrical Shell", *ASME J. of Vibration and Acoustics*, Vol. 111, pp. 337~342.

(14) Warner, J. V. and Bernhard, R. J., 1987, "Digital Control of Sound Fields in Three-dimensional Enclosure", AIAA 11th Aeroacoustics Conference-Palo Alto, California.

(15) Eriksson, L. J., Allie, M. C. and Greigner, R. A., 1987, "The Selection and Application of an IIR Adaptive Filter for Use in Active Sound Attenuation", IEEE Transaction on Acoustics, Speech and Signal Processing, pp. 433~437.

(16) Nelson, P. A. and Elliott, S. J. Active control of sound, Academic Press, 1992.

(17) Elliott, S. J., Stothers, I. M. and Nelson, P. A., 1987, "A Multiple Error LMS Algorithm and Its Application to the Active Control of Sound and Vibration", IEEE Trans. On Acoustics, Speech, and Signal Processing, Vol. ASSP-35, No. 10.

(18) Saunders, W. R., Robertshaw, H. H. and Burdisso, R. A., 1996, "A Hybrid Structural Control Approach for Narrow-band and Impulsive Disturbance Rejection", Noise Control Engineering Journal 44, pp. 11~21.

(19) Kim, Y. S., Kim, I. S. and Lee, C., 1988, "Active Noise Control in the Acoustic Rectangular Enclosure using Multiple Adaptive Feedforward Control with Feedback Loop", The Fourth International Conference on Motion and Vibration Control, pp. 467~472.

(20) Kim, Insoo., Na, Heeseung., Kim, Kwangjoon. and Park, youngjin., 1994, "constraint filtered-x and filtered-u LMS Algorithms for the Active Control of Noise in Ducts", Journal of Acoustical Society of America, Vol. 95(6), pp. 3379~3389.